



NASA 2009 Body of Knowledge (BoK) Carbon Nanotube Technology

David Gerke
Jet Propulsion Laboratory
Pasadena, California

Jet Propulsion Laboratory
California Institute of Technology
Pasadena, California

09-22 10/09



NASA 2009 Body of Knowledge (BoK) Carbon Nanotube Technology

NASA Electronic Parts and Packaging (NEPP) Program
Office of Safety and Mission Assurance
(Electronic Packaging Project)

David Gerke
Jet Propulsion Laboratory
Pasadena, California

NASA WBS: 724927.40.43
JPL Project Number: 103982
Task Number: 03.03.13

Jet Propulsion Laboratory
4800 Oak Grove Drive
Pasadena, CA 91109

<http://nepp.nasa.gov>

This research was carried out at the Jet Propulsion Laboratory, California Institute of Technology, and was sponsored by the National Aeronautics and Space Administration Electronic Parts and Packaging (NEPP) Program.

Reference herein to any specific commercial product, process, or service by trade name, trademark, manufacturer, or otherwise, does not constitute or imply its endorsement by the United States Government or the Jet Propulsion Laboratory, California Institute of Technology.

Copyright 2009. California Institute of Technology. Government sponsorship acknowledged.

ACKNOWLEDGEMENTS

The author would like to acknowledge the NASA Electronic Parts and Packaging (NEPP) Program, managed by Michael Sampson and Kenneth Label, for funding. The author would also like to thank the following individuals for their contributions to this work: Chuck Barnes and Phil Zulueta.

Table of Contents

1	Executive Summary	1
2	Introduction—What are Carbon Nanotubes?.....	1
2.1	Types of Carbon Nanotubes and Related Structures	2
2.1.1	Single-Walled Nanotubes	2
2.1.2	Multi-Walled Nanotubes.....	3
2.1.3	Fullerite	3
2.1.4	Torus	3
2.1.5	Nanobud.....	3
2.2	Synthesis—How are CNTs Made?	4
2.2.1	Arc Discharge	4
2.2.2	Laser Ablation.....	4
2.2.3	Chemical Vapor Deposition (CVD).....	5
2.2.4	Natural, Incidental, and Controlled Flame Environments	6
2.3	Properties	6
2.3.1	Strength.....	6
2.3.2	Electrical	7
2.3.3	Thermal.....	7
2.3.4	Defects	8
3	Applications of Interest.....	8
3.1	Electrical Circuits.....	8
3.2	Radiation Hardness	10
3.3	Electronic Packaging	13
3.3.1	Thermal Management	13
3.3.2	Interconnection: Chip-to-Package	15
3.3.2.1	CNT Transfer Process to Connect a Device to a Package.....	16
3.3.2.2	Electrical Performance of the CNT Interconnection	17
3.3.2.2.1	Utilizing Thermal Compression Bonding and Adhesives.....	20
3.3.2.2.2	Nonconductive Adhesives/Films.....	21
3.3.3	Electromagnetic Shielding.....	23
4	Conclusions.....	25
5	Recommendations for NASA	25
	References.....	25

1 Executive Summary

The research area of carbon nanotubes (CNTs) is a very active one. Many countries conduct research in microelectronics and, in particular, microelectronics packaging; namely, the United States (Georgia Tech), Korea, Taiwan, and Japan.

This report discusses CNTs used in microelectronics, with an emphasis on microelectronics packaging. As was discovered by performing this survey, universities primarily perform and report on research in the area of CNTs (for electronics), with only a couple of noted companies reporting on work in this area: Intel and Mitsubishi.

Work in this area appears to have reached a critical mass such that, in the near future, products will be introduced using CNTs because of the advantages this technology offers in the areas of electrical properties, extraordinary strength, and efficiency in heat conduction. For the NEPP program, CNTs offer potential future solutions to radiation hardness and electronic packaging in the areas of thermal management and interconnection.

This technology is not mature enough to start new work in the coming fiscal year (FY); therefore, no new NEPP task is recommended for FY2010.

2 Introduction—What are Carbon Nanotubes?

Carbon nanotubes (CNTs) are allotropes of carbon with a nanostructure that can have a length-to-diameter ratio of up to 28,000,000:1 [1], which is significantly larger than any other material. These cylindrical carbon molecules have novel properties that make them potentially useful in many applications in nanotechnology, electronics, optics, and other fields of materials science, as well as potential uses in architectural fields. They exhibit extraordinary strength and unique electrical properties, and are efficient conductors of heat. Their final usage, however, may be limited by their potential toxicity.

Nanotubes are members of the fullerene structural family, which also includes the spherical buckyballs. The ends of a nanotube might be capped with a hemisphere of the buckyball structure. Their name is derived from their size, since the diameter of a nanotube is on the order of a few nanometers (approximately 1/50,000th of the width of a human hair), while they can be up to several millimeters in length (as of 2008). Nanotubes are categorized as single-walled nanotubes (SWNTs) and multi-walled nanotubes (MWNTs).

The nature of the bonding of a nanotube is described by applied quantum chemistry, specifically, orbital hybridization. The chemical bonding of nanotubes is composed entirely of sp^2 bonds, similar to those of graphite. This bonding structure, which is stronger than the sp^3 bonds found in diamonds, provides the molecules with their unique strength. Nanotubes naturally align themselves into “ropes” held together by Van der Waals forces. Under high pressure, nanotubes can merge together, trading some sp^2 bonds for sp^3 bonds, giving the possibility of producing strong, unlimited-length wires through high-pressure nanotube linking.

2.1 Types of Carbon Nanotubes and Related Structures

2.1.1 Single-Walled Nanotubes

Most SWNTs have a diameter of close to 1 nanometer, with a tube length that can be many thousands of times longer. The structure of a SWNT can be conceptualized by wrapping a one-atom-thick layer of graphite called graphene into a seamless cylinder. The way the graphene sheet is wrapped is represented by a pair of indices (n,m) called the chiral vector. The integers n and m denote the number of unit vectors along two directions in the honeycomb crystal lattice of graphene. If $m=0$, the nanotubes are called “zigzag.” If $n=m$, the nanotubes are called “armchair.” Otherwise, they are called “chiral.”

SWNTs are an important variety of carbon nanotube because they exhibit electric properties that are not shared by the MWNT variants. SWNTs are the most likely candidate for miniaturizing electronics beyond the micro-electromechanical scale currently used in electronics. The most basic building block of these systems is the electric wire, and SWNTs can be excellent conductors [2,3]. One useful application of SWNTs is in the development of the first intramolecular field effect transistors (FET). Production of the first intramolecular logic gate using SWNT FETs has recently become possible as well [4]. To create a logic gate, you must have both a p-FET and an n-FET. Because SWNTs are p-FETs when exposed to oxygen and n-FETs otherwise, it is possible to protect half of an SWNT from oxygen exposure, while exposing the other half to oxygen. This results in a single SWNT that acts as a NOT logic gate with both p and n-type FETs within the same molecule. Examples of SWNTs are illustrated in Figure 2-1.

The development of affordable synthesis techniques is vital to the future of carbon nanotechnology. Several suppliers offer as-produced arc discharge SWNTs for ~\$50–\$100 per gram as of 2007 [6,7].

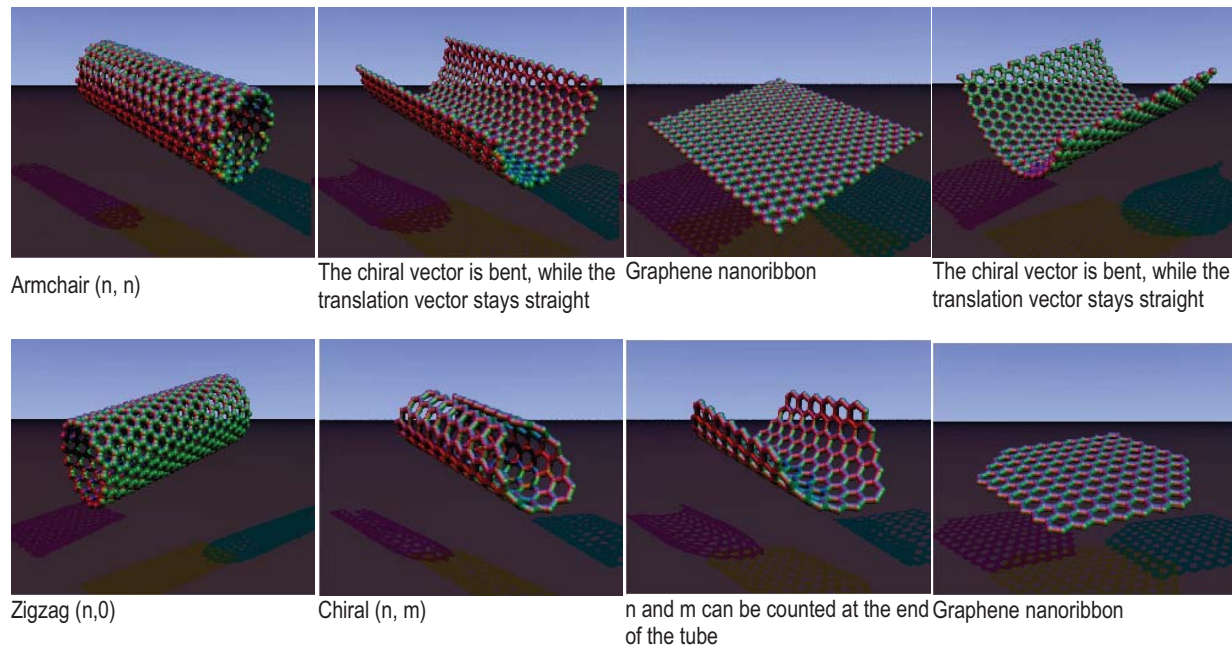


Figure 2-1. Single-walled nanotubes (SWNTs).

2.1.2 Multi-Walled Nanotubes

MWNTs consist of multiple layers of rolled graphite that form a tube shape. There are two models that can be used to describe the structures of MWNT. In the *Russian Doll* model, sheets of graphite are arranged in concentric cylinders, e.g., a (0,8) SWNT within a larger (0,10) SWNT. In the *Parchment* model, a single sheet of graphite is rolled around itself, resembling a scroll of parchment or a rolled newspaper. The interlayer distance in MWNTs is close to the distance between graphene layers in graphite, approximately 3.3 Å (330 pm).

The special place of double-walled carbon nanotubes (DWNT) must be emphasized here because their morphology and properties are similar to SWNT, but their resistance to chemicals is significantly improved. This is especially important when functionalization is required (this means grafting of chemical functions at the surface of the nanotubes) to add new properties to the CNT. In the case of SWNT, covalent functionalization will break some C=C double bonds, leaving “holes” in the structure of the nanotube and thus modifying both its mechanical and electrical properties. In the case of DWNT, only the outer wall is modified. DWNT synthesis on the gram-scale was first proposed in 2003 by the Combustion Chemical Vapor Deposition (CCVD) technique, from the selective reduction of oxide solutions in methane and hydrogen [8].

2.1.3 Fullerite

Fullerites are the solid-state manifestations of fullerenes and related compounds and materials. Being highly incompressible nanotube forms, polymerized single-walled nanotubes (P-SWNT) are a class of fullerites and are comparable to diamond in terms of hardness. However, due to the way that nanotubes intertwine, P-SWNTs do not have the corresponding crystal lattice that makes it possible to cut diamonds neatly. This same structure results in a less brittle material, as any impact that the structure would sustain can be spread across the material.

2.1.4 Torus

A nanotorus is a theoretically described carbon nanotube bent into a torus (doughnut shape). Nanotori have many unique properties, such as magnetic moments 1000 times larger than previously expected for certain specific radii [8]. Properties such as magnetic moment and thermal stability vary widely depending on radius of the torus and radius of the tube [9,10].

2.1.5 Nanobud

Carbon nanobuds are a newly created material combining two previously discovered allotropes of carbon—CNTs and fullerenes (see Figure 2-2). In this new material, fullerene-like “buds” are covalently bonded to the outer sidewalls of the underlying carbon nanotube. This hybrid material has useful properties of both fullerenes and CNTs. In particular, they have been found to be exceptionally good field emitters. In composite materials, the attached fullerene molecules may function as molecular anchors preventing slipping of the nanotubes, thus improving the composite’s mechanical properties.



Figure 2-2. A stable nanobud structure

2.2 Synthesis—How are CNTs Made?

Techniques have been developed to produce nanotubes in sizeable quantities, including arc discharge [11], laser ablation [14], high pressure carbon monoxide (HiPCO) [5], and chemical vapor deposition (CVD) [20, 21]. Most of these processes take place in vacuum or with process gases. CVD growth of CNTs can occur in vacuum or at atmospheric pressure. Large quantities of nanotubes can be synthesized by these methods; advances in catalysis and continuous growth processes are making CNTs more commercially viable.

2.2.1 Arc Discharge

Nanotubes were observed in 1991 in the carbon soot of graphite electrodes during an arc discharge, by using a current of 100 amps, which was intended to produce fullerenes [11]. However, the first macroscopic production of CNTs was made in 1992 by two researchers at NEC's Fundamental Research Laboratory [12]. The method used was the same as in 1991. During this process, the carbon contained in the negative electrode sublimates because of the high discharge temperatures. Because nanotubes were initially discovered using this technique, it has been the most widely used method of nanotube synthesis.

The yield for this method is up to 30 percent by weight and produces both SWNTs and MWNTs with lengths of up to 50 micrometers [5].

2.2.2 Laser Ablation

In the laser ablation process, a pulsed laser vaporizes a graphite target in a high-temperature reactor while an inert gas is bled into the chamber. Nanotubes develop on the cooler surfaces of the reactor as the vaporized carbon condenses. A water-cooled surface may be included in the system to collect the nanotubes.

This process was developed by Dr. Richard Smalley and co-workers at Rice University, who at the time of the discovery of CNTs, were blasting metals with a laser to produce various metal molecules. When they heard of the existence of nanotubes, they replaced the metals with graphite to create multi-walled carbon nanotubes [13]. Later that year, the team used a composite of graphite and metal catalyst particles (the best yield was from a cobalt and nickel mixture) to synthesize single-walled carbon nanotubes [14].

The laser ablation method yields around 70% and produces primarily single-walled carbon nanotubes with a controllable diameter determined by the reaction temperature. However, it is more expensive than either arc discharge or chemical vapor deposition [5].

2.2.3 Chemical Vapor Deposition (CVD)

The catalytic vapor phase deposition of carbon was first reported in 1959 [15], but it was not until 1993 [16] that CNTs were formed by this process. In 2007, researchers at the University of Cincinnati (UC) developed a process to grow aligned carbon nanotube arrays of 18-mm length on a FirstNano ET3000 carbon nanotube growth system [17].

During chemical vapor deposition (CVD), a substrate is prepared with a layer of metal catalyst particles, most commonly nickel, cobalt [18], iron, or a combination of the three [19]. The metal nanoparticles can also be produced other ways, including reduction of oxides or oxide solid solutions. The diameters of the nanotubes that are to be grown are related to the size of the metal particles. This can be controlled by patterned (or masked) deposition of the metal, annealing, or by plasma etching of a metal layer. The substrate is heated to approximately 700°C. To initiate the growth of nanotubes, two gases are bled into the reactor: a process gas (such as ammonia, nitrogen or hydrogen) and a carbon-containing gas (such as acetylene, ethylene, ethanol, or methane). Nanotubes grow at the sites of the metal catalyst; the carbon-containing gas is broken apart at the surface of the catalyst particle, and the carbon is transported to the edges of the particle where it forms the nanotubes. This mechanism is still being studied [20]. The catalyst particles can stay at the tips of the growing nanotube during the growth process or remain at the nanotube base, depending on the adhesion between the catalyst particle and the substrate.

CVD is a common method for the commercial production of CNTs. For this purpose, the metal nanoparticles are mixed with a catalyst support such as MgO or Al₂O₃ to increase the surface area for higher yield of the catalytic reaction of the carbon feedstock with the metal particles. One issue in this synthesis route is the removal of the catalyst support via an acid treatment, which sometimes could destroy the original structure of the CNTs. However, alternative catalyst supports that are soluble in water have proven effective for nanotube growth [20].

If a plasma is generated by the application of a strong electric field during the growth process (plasma enhanced chemical vapor deposition), then the nanotube growth will follow the direction of the electric field [21]. By adjusting the geometry of the reactor, it is possible to synthesize vertically aligned CNTs (i.e., perpendicular to the substrate), a morphology that has been of interest to researchers interested in the electron emission from nanotubes. Without the plasma, the resulting nanotubes are often randomly oriented. Under certain reaction conditions, even in the absence of a plasma, closely spaced nanotubes will maintain a vertical growth direction resulting in a dense array of tubes resembling a carpet or forest [21].

Of the various means for nanotube synthesis, CVD shows the most promise for industrial-scale deposition, because of its price/unit ratio, and because CVD is capable of growing nanotubes directly on a desired substrate, whereas the nanotubes must be collected in the other growth techniques. The growth sites are controllable by careful deposition of the catalyst. In 2007, a team from Meijo University demonstrated a high-efficiency CVD technique for growing CNTs

from camphor [22]. Researchers at Rice University, until recently led by the late Dr. Richard Smalley, have concentrated upon finding methods to produce large, pure amounts of particular types of nanotubes. Their approach grows long fibers from many small seeds cut from a single nanotube; all of the resulting fibers were found to be of the same diameter as the original nanotube and were expected to be of the same type as the original nanotube. Further characterization of the resulting nanotubes and improvements in yield and length of grown tubes are needed [23].

CVD growth of MWNTs is used by several companies to produce materials on the ton scale, including NanoLab [24], Bayer, Arkema, Nanocyl, Nanothinx [25], Hyperion Catalysis, Mitsui, and Showa Denko.

2.2.4 Natural, Incidental, and Controlled Flame Environments

Fullerenes and CNTs are not necessarily products of high-tech laboratories; they are commonly formed in such mundane places as ordinary flames [26]; produced by burning methane [27], ethylene [28], and benzene [29]; and found in soot from both indoor and outdoor air [30]. However, these naturally occurring varieties can be highly irregular in size and quality because the environment in which they are produced is often highly uncontrolled. Thus, although they can be used in some applications, they can lack in the high degree of uniformity necessary to meet many needs of both research and industry. Recent efforts have focused on producing more uniform CNTs in controlled flame environments [31–34]. Nano-C, Inc. of Westwood, Massachusetts, is producing flame-synthesized, single-walled carbon nanotubes. This method has promise for large-scale, low-cost nanotube synthesis, though it must compete with rapidly developing large-scale CVD production.

2.3 Properties

2.3.1 Strength

CNTs are the strongest and stiffest materials yet discovered in terms of tensile strength and elastic modulus, respectively. This strength results from the covalent sp^2 bonds formed between the individual carbon atoms. In 2000, a multi-walled carbon nanotube was tested to have a tensile strength of 150 gigapascals (GPa) [35]. (This, for illustration, translates into the ability to endure a weight of 15,000 kg on a cable with cross-section of 1 mm^2 .) Since CNTs have a low density for a solid of $1.3\text{--}1.4 \text{ g}\cdot\text{cm}^{-3}$ [35], its specific strength of up to $48,000 \text{ kN}\cdot\text{m}\cdot\text{kg}^{-1}$ is the best of known materials, compared to high-carbon steel's $154 \text{ kN}\cdot\text{m}\cdot\text{kg}^{-1}$.

Under excessive tensile strain, the tubes will undergo plastic deformation, which means the deformation is permanent. This deformation begins at strains of approximately 5% and can increase the maximum strain the tubes undergo before fracture by releasing strain energy.

Table 2-1. Comparison of mechanical properties [36–42].

Material	Young's Modulus (TPa)	Tensile Strength (GPa)	Elongation at Break (%)
SWNT	~1 (from 1 to 5)	13–53 ^E	16
Armchair SWNT	0.94 ^T	126.2 ^T	23.1
Zigzag SWNT	0.94 ^T	94.5 ^T	15.6–17.5
Chiral SWNT	0.92		
MWNT	0.8–0.9 ^E	150	
<u>Stainless Steel</u>	~0.2	~0.65–1	15–50
<u>Kevlar</u>	~0.15	~3.5	~2
Kevlar ^T	0.25	29.6	

^EExperimental observation^TTheoretical prediction

CNTs are not nearly as strong under compression. Because of their hollow structure and high aspect ratio, they tend to undergo buckling when placed under compressive, torsional or bending stress. Table 2-1 contains comparisons of various types of CNTs and structural materials.

The above discussion referred to axial properties of the nanotube, whereas simple geometrical considerations suggest that CNTs should be much softer in the radial direction than along the tube axis. Transmission Electron Microscopy (TEM) observation of radial elasticity suggests that even the Van der Waals forces can deform two adjacent nanotubes [43]. Nanoindentation experiments, performed by several groups on multi-walled CNTs, indicates Young's modulus of the order of several Gpa, confirming that CNTs are indeed rather soft in the radial direction [44,45].

2.3.2 Electrical

Because of the symmetry and unique electronic structure of graphene, the structure of a nanotube strongly affects its electrical properties. For a given (n,m) nanotube, if $n = m$, the nanotube is metallic; if $n - m$ is a multiple of 3, then the nanotube is semiconducting with a very small band gap; otherwise, the nanotube is a moderate semiconductor. Thus, all armchair ($n=m$) nanotubes are metallic, and nanotubes (5,0), (6,4), (9,1), etc. are semiconducting. In theory, metallic nanotubes can carry an electrical current density of 4×10^9 A/cm² which is more than 1,000 times greater than metals such as copper [46].

2.3.3 Thermal

All nanotubes are expected to be very good thermal conductors along the tube (exhibiting a property known as “ballistic conduction”), but good insulators laterally to the tube axis. It is predicted that CNTs will be able to transmit up to 6000 watts per meter per Kelvin (K) at room temperature; compare this to copper, a metal well-known for its good thermal conductivity, which transmits 385 watts per meter per K. The temperature stability of CNTs is estimated to be up to 2800°C in vacuum and about 750°C in air.

2.3.4 Defects

As with any material, the existence of a crystallographic defect affects the material properties. Defects can occur in the form of atomic vacancies. High levels of such defects can lower the tensile strength by up to 85%. Another form of carbon nanotube defect is the Stone Wales defect, which creates a pentagon and heptagon pair by rearrangement of the bonds. Because of the very small structure of CNTs, the tensile strength of the tube is dependent on its weakest segment in a similar manner to a chain, where the strength of the weakest link becomes the maximum strength of the chain.

Crystallographic defects also affect the tube's electrical properties. A common result is lowered conductivity through the defective region of the tube. A defect in armchair-type tubes (which can conduct electricity) can cause the surrounding region to become semiconducting, and single monoatomic vacancies induce magnetic properties [47].

Crystallographic defects strongly affect the tube's thermal properties. Such defects lead to phonon scattering, which in turn increases the relaxation rate of the phonons. This reduces the mean free path and reduces the thermal conductivity of nanotube structures. Phonon transport simulations indicate that substitutional defects such as nitrogen or boron will primarily lead to scattering of high-frequency optical phonons. However, larger-scale defects such as Stone Wales defects cause phonon scattering over a wide range of frequencies, leading to a greater reduction in thermal conductivity [46].

3 Applications of Interest

As with most new materials, there is an almost endless list of new possible applications for carbon nanotubes (CNTs)—clothes, concrete, solar cells, hydrogen storage, electrical parts, and packaging. This effort is funded to report on applications in electronic packaging; therefore, the remainder of this report will touch upon the use of CNTs in electronic parts and focus on the available electronic packaging applications.

3.1 Electrical Circuits

CNTs can, in principle, play the same role as silicon in electronic circuits, but at a molecular scale where silicon and other standard semiconductors cease to work. Although the electronics industry is already pushing the critical dimensions of transistors in commercial chips below 200 nanometers—approximately 400 atoms wide—engineers face large obstacles in continuing this miniaturization [5].

A nanotube formed by joining nanotubes of two different diameters end to end can act as a diode, suggesting the possibility of constructing electronic computer circuits entirely out of nanotubes. Because of their good thermal properties, CNTs can also be used to dissipate heat from tiny computer chips. The longest electricity-conducting circuit is a fraction of an inch long [47].

Fabrication difficulties are major hurdles for CNTs to find prominent places in circuits. The production of electrical circuits with CNTs is very different from the traditional integrated circuit (IC) fabrication process. Films are deposited onto a wafer and pattern-etched away.

However they form, the composition and geometry of CNTs engender a unique electronic complexity. That is, in part, simply the result of size, because quantum physics governs at the nanometer scale. But graphite itself is a very unusual material. Whereas most electrical conductors can be classified as either metals or semiconductors, graphite is one of the rare materials known as a semimetal, delicately balanced in the transitional zone between the two. By combining graphite's semimetallic properties with the quantum rules of energy levels and electron waves, CNTs emerge as tunable conductors.

For example, one rule of the quantum world is that electrons behave like waves as well as particles, and electron waves can reinforce or cancel one another. As a consequence, an electron spreading around a nanotube's circumference can completely cancel itself out; thus, only electrons with just the right wavelength remain. Out of all the possible electron wavelengths, or quantum states, available in a flat graphite sheet, only a tiny subset is allowed when we roll that sheet into a nanotube. That subset depends on the circumference of the nanotube, as well as whether the nanotube twists like a barbershop pole.

Slicing a few electron states from a simple metal or semiconductor will not produce many surprises, but semimetals are much more sensitive materials, and that is where CNTs become interesting. In a graphite sheet, one particular electron state (which physicists call the Fermi point) gives graphite almost all of its conductivity; none of the electrons in other states are free to move about. Only one third of all CNTs combine the right diameter and degree of twist to include this special Fermi point in their subset of allowed states. These nanotubes are truly metallic nanowires.

The remaining two thirds of nanotubes are semiconductors. That means that, like silicon, they do not pass current easily without an additional boost of energy. A burst of light or a voltage can knock electrons from valence states into conducting states where they can move about freely. The amount of energy needed depends on the separation between the two levels and is the so-called band gap of a semiconductor. It is semiconductors' band gaps that make them so useful in circuits, and by having a library of materials with different band gaps, engineers have been able to produce the vast array of electronic devices available today.

Figure 3-1 illustrates field-effect transistors (FETs) using single semiconducting nanotubes between two metal electrodes as a channel through which electrons flow. The current flowing in the channel can be switched on or off by applying voltages to a nearby third electrode. The nanotube-based devices operate at room temperature with electrical characteristics similar to off-the-shelf silicon devices. In these devices, the gate electrode can change the conductivity of the nanotube channel in an FET by a factor of one million or more, comparable to silicon FETs. Because of its tiny size, the nanotube FET switches reliably use much less power than a silicon-based device. Theorists predict that a truly nanoscale switch could run at clock speeds of one terahertz or more—1,000 times as fast as processors available today.

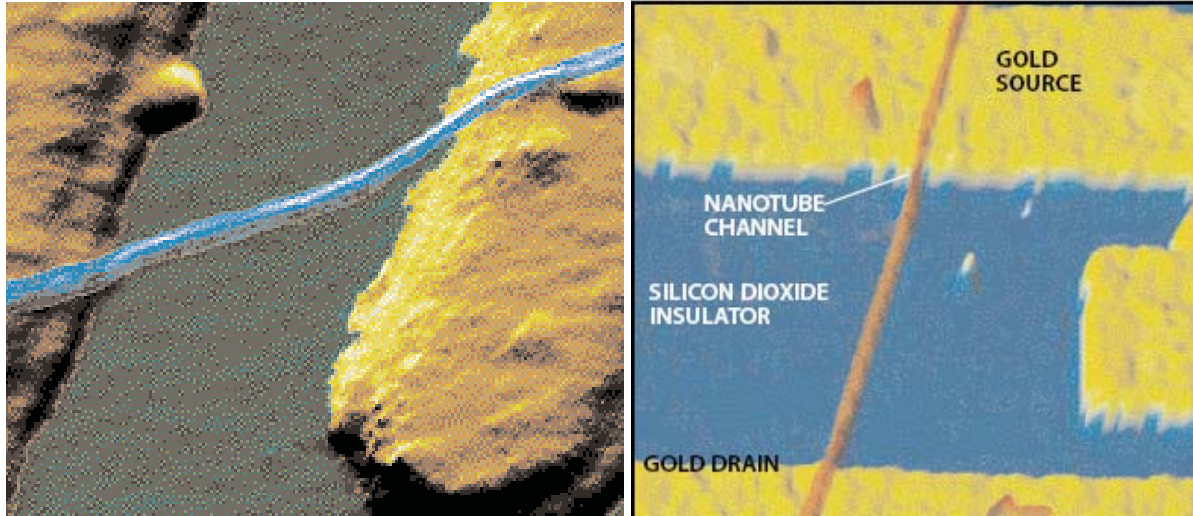


Figure 3-1. Electrically conductive macromolecules of carbon that self-assemble into tubes have been tested as ultrafine wires (*left*) and as channels in experimental field-effect transistors (*right*) [5].

The fact that nanotubes come with a variety of band gaps and conductivities raises many intriguing possibilities for additional nanodevices. Joined metallic and semiconducting nanotubes have shown that such junctions behave as diodes, permitting electricity to flow in only one direction. Theoretically, combinations of nanotubes with different band gaps could behave like light-emitting diodes and perhaps even nanoscopic lasers. It is now possible to build a nanocircuit that has wires, switches, and memory elements made entirely from nanotubes and other molecules.

3.2 Radiation Hardness

The electrical properties of CNTs are strongly dependent on their atomic structures—a nanotube can be metallic or semiconducting depending on the chirality vector (n,m) that defines the diameter and the chiral angle of a CNT [2]. Furthermore, the electrical properties of CNTs are extremely sensitive to defects, which can be introduced during the growth by mechanical strain or by irradiation with energetic particles such as electrons, heavy ions, alpha-particles, and protons.

The effects of electron and heavy-ion irradiation on CNTs have been reported [48–50]. A controlled irradiation on CNTs might be a method for modifying the physical and chemical properties of CNTs by introducing structural defects into the side walls. On the other hand, when highly energetic particles collide, a latchup, electrical interference, charging, sputtering, erosion, and puncture of the target device can occur. As a result, degradation of the device performance and lifetime or even a system failure of the underlying electronics may occur.

To understand the effects of various types of irradiation on CNT-based devices in aerospace radiation environments, Woong-Ki Hong et al. [51] studied the effects of proton irradiation on the electrical properties of CNT-network FET devices showing metallic or semiconducting behaviors. The CNT-FET devices were exposed to 10–35 MeV proton beams with a fluence of $4 \times 10^{10} - 4 \times 10^{12} \text{ cm}^{-2}$ that are comparable to the aerospace environment. They also performed micro-Raman spectroscopy directly on the CNT-FET devices to correlate the structural changes

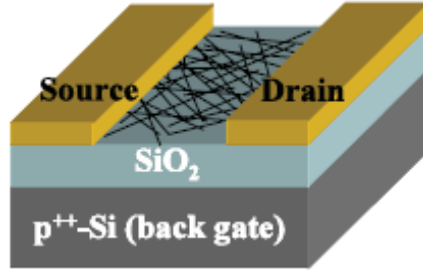


Figure 3-2. Schematic drawing of single-walled carbon nanotube network field effect transistor (SWNT network FET) [52].

to any potential electrical property changes in CNTs under proton irradiation. Proton implant effects were modeled using SRIM-2003 (stopping and range of ions into matter).

In Woong-Ki Hong's work, the CNT-network FET devices used single-walled carbon nanotubes (SWNTs) produced by an arc-discharge process (commercially available from Iljin Nanotech Co., Ltd, Korea) [52]. The SWNTs were purified and a suspension was dropped on a 100-nm or a 300-nm thick thermally grown oxide on silicon. The silicon substrate was a highly doped p-type substrate that was used as a back gate. Metal electrodes consisting of Ti (30 nm)/Au (60 nm) were then deposited by an electron-beam evaporator and defined as the source and drain electrodes by photolithography and a lift-off process. The distance between the source and drain electrodes was 2–3 μm . Figure 3-2 shows a schematic diagram of a fabricated SWNT-network FET device.

Accelerated proton beams were generated using a MC-50 cyclotron (at the Korea Institute of Radiological and Medical Sciences). The beam diameter was ~ 6 cm, its uniformity was $\sim 90\%$, and the average beam current was 10 nA. Three different proton beam energies were used: 10, 20, and 35 MeV. The total fluences during the proton irradiation were $1.2 \times 10^{11} - 1.4 \times 10^{12} \text{ cm}^{-2}$ for 10 and 20 MeV and $4.1 \times 10^{10} - 4.1 \times 10^{12} \text{ cm}^{-2}$ for 35 MeV [53]. The irradiation time of the proton beams was varied from 60 to 6000 s. The 30–60 MeV protons at a dose of $\sim 10^{12} \text{ cm}^{-2}$ are equivalent to an amount of proton radiation for a few hundred years in a low Earth orbit environment [53].

Figures 3-3 and 3-4 show representative data for the SWNT-network FET devices, which show metallic or weak-metallic (weak-semiconducting) behaviors before and after proton irradiation. These figures are the transfer characteristics of an SWNT-network FET device before and after proton irradiation at 10 and 35 MeV, respectively. The irradiation time and the fluence for the devices shown in Figures 3-3 and 3-4 were 1800 and 600 s, 6.9×10^{11} and $4.1 \times 10^{11} \text{ cm}^{-2}$ for 10 and 35 MeV, respectively.

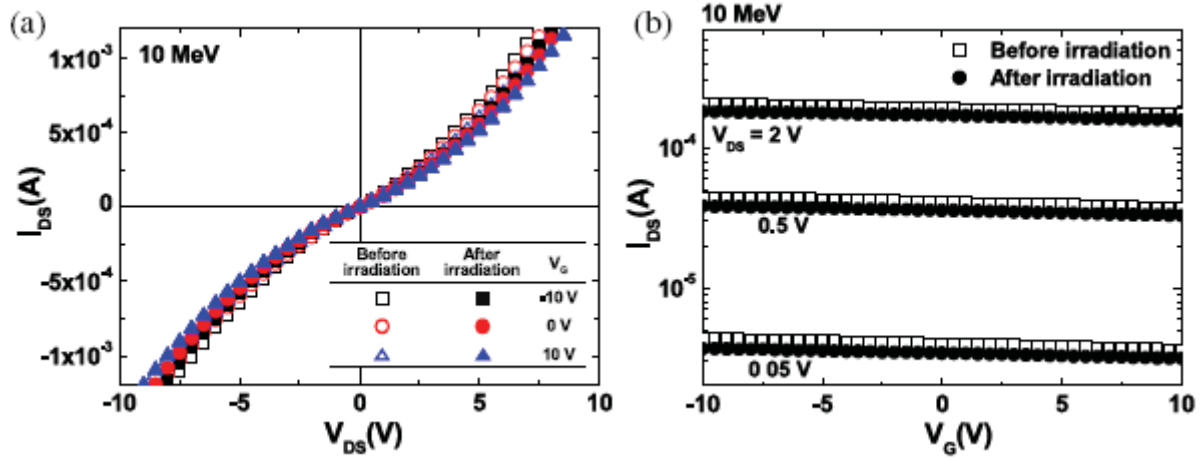


Figure 3-3. Transfer characteristics of metallic SWNT-network FETs before and after proton irradiation at 10 MeV and a fluence of $1.4 \times 10^{12} \text{ cm}^{-2}$. (a) Source-drain current versus drain voltage at various gate voltages ($V_G = -10, 0,$ and 10 V). (b) Source-drain current as a function of gate voltage at various source-drain biases ($V_{DS} = 0.05, 0.5,$ and 2 V) [52].

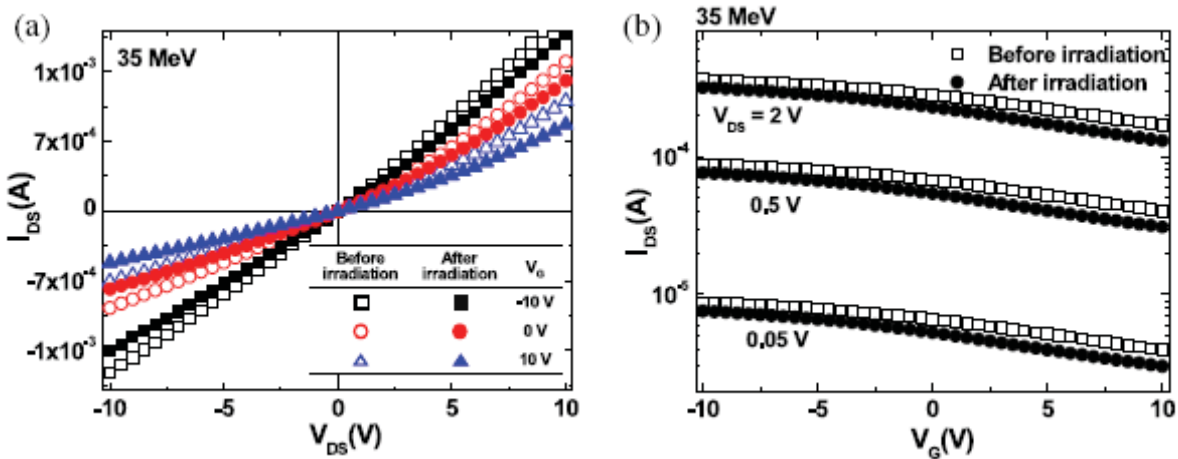


Figure 3-4. Transfer characteristics of weak-metallic SWNT network FETs before and after proton irradiation at 35 MeV and a fluence of $4.1 \times 10^{11} \text{ cm}^{-2}$. (a) Source-drain current versus drain voltage at various gate voltages ($V_G = -10, 0,$ and 10 V). (b) Source-drain current as a function of gate voltage at various source-drain biases ($V_{DS} = 0.05, 0.5,$ and 2 V) [52].

Figure 3-5 shows the semi-conductive electrical properties of irradiated SWNT-network FET devices. These particular devices show p-type semiconducting behavior, since the current increases with increasing negative gate voltage, whereas it decreases down to a few pico amperes (pA) with increasing positive gate voltage. The ratio of the current change (I_{on}/I_{off}) was over 105 at $V_{DS} = 0.5$ V while the gate voltage was swept from -6 to 6 V. Similarly, to the metallic and weak-metallic SWNT-network FET devices (Figures 3-3 and 3-4), the electrical transport properties of the semiconducting SWNT-network FET were not influenced by the proton irradiation (Figure 3-5). These electrical results along with Raman Spectroscopy data indicate that CNT-network FET devices are very tolerant under proton beam conditions, which are comparable to an aerospace environment, and suggest a radiation hardness of CNT-related electronic devices when used in outer space [52].

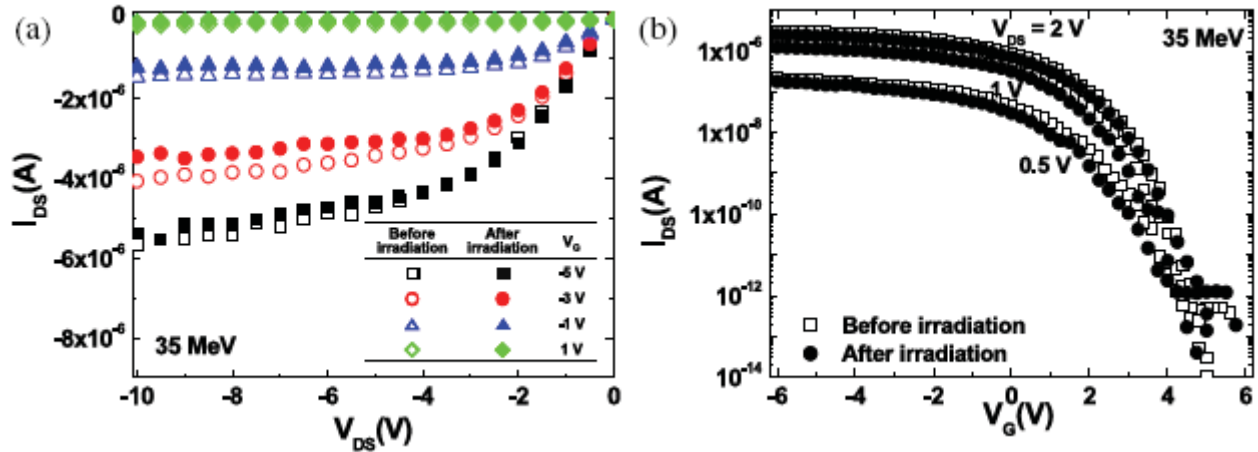


Figure 3-5. Transfer characteristics of semiconducting SWNT-network FETs before and after proton irradiation with energy of 35 MeV and fluence of $4.1 \times 10^{12} \text{ cm}^{-2}$. (a) Source-drain current versus drain voltage at various gate voltages ($V_G = -5, -3, -1,$ and 1 V). (b) Source-drain current as a function of gate voltage at various source-drain biases ($V_{DS} = 0.5, 1,$ and 2 V) [52].

3.3 Electronic Packaging

Electronic packaging is one of the key enabling technologies for the microelectronics industry. As the performance of semiconductor products increases, the technical challenges increase in areas of power delivery, heat removal, input/output (I/O) density, and thermomechanical reliability.

3.3.1 Thermal Management

As IC performance increases, many technical challenges appear in the areas of thermal management and thermal-mechanical reliability. To address these issues, aligned CNTs are being used in IC packaging as thermal interface materials. These materials, which are sandwiched between silicon chips and the metal heat sinks, fill gaps and irregularities between the chip and metal surfaces to enhance heat flow between the two. Recent findings have shown that the nanotube-based interfaces can conduct several times more heat than conventional thermal interface materials at the same temperatures [55,56].

Nanotubes can range in diameter from less than one nanometer to approximately 100 nanometers. CNTs can be grown in an aligned fashion, which is generally referred to as aligned carbon nanotubes (ACNTs). Figure 3-6 shows SEM images of ACNT pillars with different growth times.

All the SEM images in Figure 3-6 show that nearly vertical-aligned CNT pillars can be formed on a substrate without any entanglement with neighboring CNTs. The controlled growth of CNTs at different levels is possible by controlling the reaction chemistry and growth condition. The vertical alignment of ACNT pillars is also influenced by their aspect ratio. As shown in Figure 3-6c, the CNT pillars with high aspect ratio (~ 15) tend to bend over a few degrees. Typically, the ACNT pillars can be manufactured so that they are vertically aligned with an aspect ratio up to 5. Such height and aspect ratio can satisfy most interconnect applications.

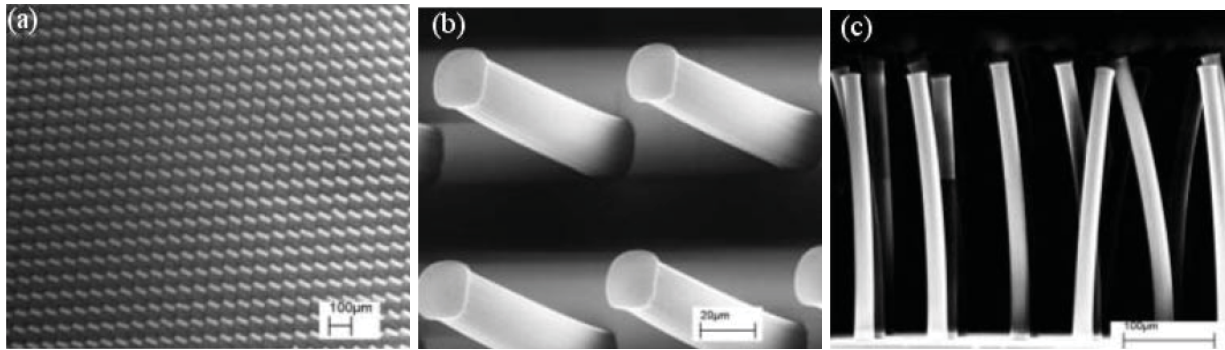


Figure 3-6. SEM images of (a) as-grown ACNT pillars on 20 µm catalyst islands; (b) magnified image of (a); (c) high aspect ratio CNT pillars [56].

Using CNTs grown to a controlled length, a Velcro[®]-like nanocarpet, which fits between two thermal interfaces, can be manufactured. The nanocarpet, called a “carbon nanotube array thermal interface,” can be attached to both the chip and heat sink surfaces [55,56]. The term Velcro[®] is used because the structure creates an interwoven mesh of fibers when both sides of the interface are coated with nanotubes. There is not a strong mechanical bond (as implied by the term Velcro[®]), but the two pieces come together in such a way that they facilitate heat flow becoming the thermal equivalent of Velcro[®]).

The above described technique was funded by Purdue University’s Cooling Technologies Research Center, supported by the National Science Foundation, industry, and Purdue, to help corporations develop miniature cooling technologies for a wide range of applications, from electronics and computers to telecommunications and advanced aircraft. Applications in power electronics are being supported by the Air Force Research Laboratory in association with the Birck Nanotechnology Center at Purdue’s Discovery Park. The technology is ready for commercialization and is being pursued by several corporate members of the cooling research center, including Nanoconduction Inc., a startup company in Sunnyvale, California, which is a new member of the cooling center [55].

To demonstrate the feasibility of ACNT pillars as chip-to-module interconnection, solderability studies have been conducted [56]. In one study, the ACNT pillars were placed onto a thin layer of 63Sn/37Pb solder paste on copper-laminated substrates. Following a reflow cycle in a production-like seven-zone reflow oven, the interface between CNT and solder was characterized by the SEM. Dujardin et al. reported that there is an upper limit for the surface tension of the liquid (~180 mN/m) to wet the multi-walled CNTs [57]. The surface tension of eutectic Sn/Pb at 220°C is approximately 520 mN/m. However, wetting of CNTs by solder was observed, as shown in Figure 3-7. It is believed that the solder metals react with the oxygen and/or carbon to form a compound with sufficiently low surface tension to be drawn in by capillary force [58].

The preliminary wetting results showed that the ACNTs can be wetted by the molten solder, indicating the feasibility of this novel structure for chip-to-module interconnects. The highly aligned CNTs can be used as a thermal interface material for thermal managements of ultra-fast devices that dissipate high heat flux as well.

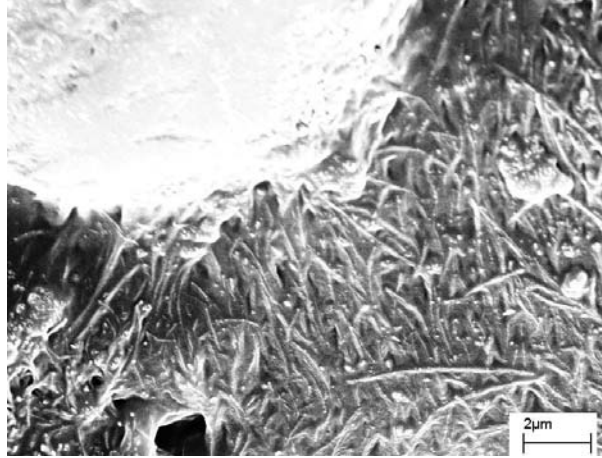


Figure 3-7. SEM micrograph of wetting of eutectic Sn/Pb on ACNTs

3.3.2 Interconnection: Chip-to-Package

High-density interconnection between a device and the microelectronic packaging that connects it to the outside world is increasingly becoming flip-chip with metallic bumps attached to the device that are connected to the package (usually by solder). Downscaling the traditional solder bump interconnect does not satisfy the thermomechanical reliability requirements at very fine distances between I/O on the order of 30 μm or less [59]. A combination of pitch-size reduction, mechanical stress concerns, and high current density requirements drives the development, process, and design of interconnect materials into entirely new directions.

CNTs are a type of novel material attracting great attention due to their outstanding thermal, electrical, and mechanical properties. These properties make them a promising alternative to metals as the interconnect materials for electronic packaging applications.

As described in previous sections of this report, there are numerous ways to grow CNTs; however, methods such as chemical vapor deposition (CVD) usually require temperatures above 600°C, which is much higher than typical packaging process temperatures. These high temperatures can damage silicon chips and organic-based substrates. Another obstacle remaining for device realization using this method is the difficulty in achieving ohmic contact between CNT arrays and electrodes. It has been found that the contact resistance between as-grown CNTs and a metal substrate can be as high as around 5 M Ω , which is too high for interconnect applications [60].

A rapid thermal annealing method at 500°C or 800°C has been used to form a carbide compound between the CNT and metal substrate in order to improve the contact properties of the CNT/metal [61,62]. However, the high processing temperature remains an issue for device packaging applications. Due to the disadvantages of high processing temperature, poor adhesion, and high contact resistance, as-grown CNTs cannot be directly used as interconnects on the chip. Therefore, a microelectronics-compatible process that is able to assemble the aligned CNT arrays on the silicon chip is needed in order to replace metal interconnects.

3.3.2.1 CNT Transfer Process to Connect a Device to a Package

The following process is a description of a flip-chip process using CNTs [63]. Aligned open-ended CNT films were transferred onto copper substrates using a technology in which eutectic tin/lead solders provide an adhesion layer [64]. This process can overcome the serious obstacles to the integration of CNTs into integrated circuits and microelectronic device packages by offering low processing temperatures and improved adhesion of CNTs to substrates. The transferred CNTs can form the mechanical and electrical connections between chips and substrates.

Tin/lead (63%Sn-37%Pb) eutectic solder metal used as an adhesion layer to transfer CNT arrays from silicon wafers to copper substrates requires an under bump metallurgy (UBM) layer before the tin-lead metal layer deposition. Eutectic solder paste coating the UBM layer with a thickness of around 200 μm forms a Sn-Pb alloy metal layer following reflow at 220°C for 10 min, which melts the solder paste. Following a cooling process, the solder metal thickness is reduced to around 10 μm following a mechanical polish. Thereafter, the silicon wafer with the CNT arrays can then be flipped over and placed on a clean copper substrate. The CNTs can then be soldered onto the substrate by utilizing a seven-zone BTU reflow oven with a nitrogen atmosphere.

Figure 3-8a shows the type of CNTs used for the transfer process. Figure 3-8b shows an SEM image of the transferred CNT arrays onto the copper substrate via Sn-Pb solders, which clearly shows that the CNT arrays were successfully transferred onto the copper substrate, and the original aligned structures of the transferred CNTs were still maintained [63].

In this instance, a Cu substrate was chosen in order to obtain a bottom electrode for electrical measurement. A similar method can be applied to many other substrates, including silicon chip, organic substrate, glass, flexible substrate, etc. Figure 3-9 proposes the process to transfer a CNT interconnect to a silicon IC chip, which makes it feasible to use CNTs to replace metal solders as interconnections [63].

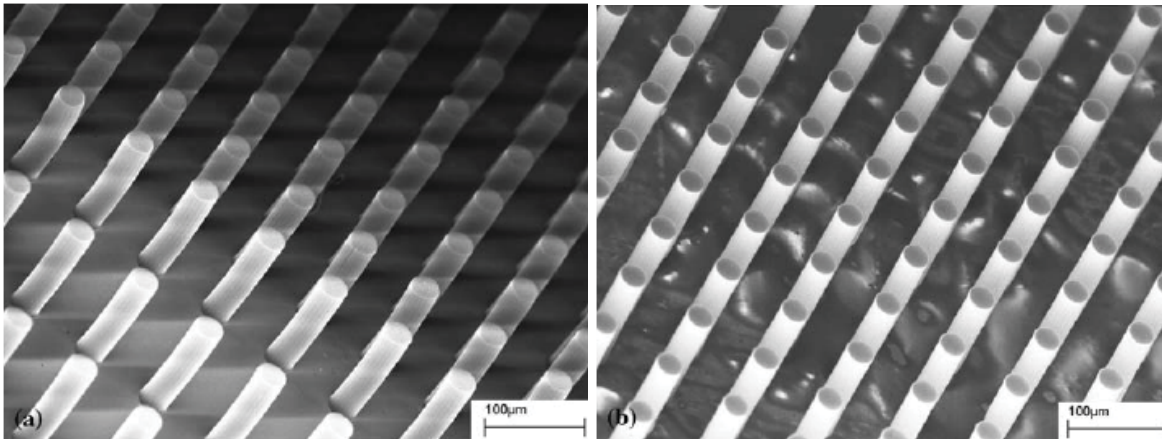


Figure 3-8. SEM images of (a) the as-synthesized CNT arrays on a Si substrate and (b) as-transferred CNT arrays on a Cu surface via Sn-Pb solders [63].

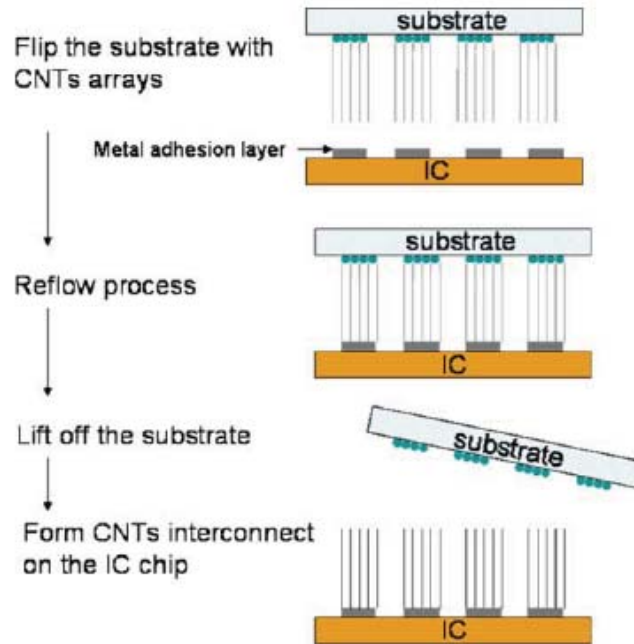


Figure 3-9. Transfer method to form CNT interconnects on the chip [63].

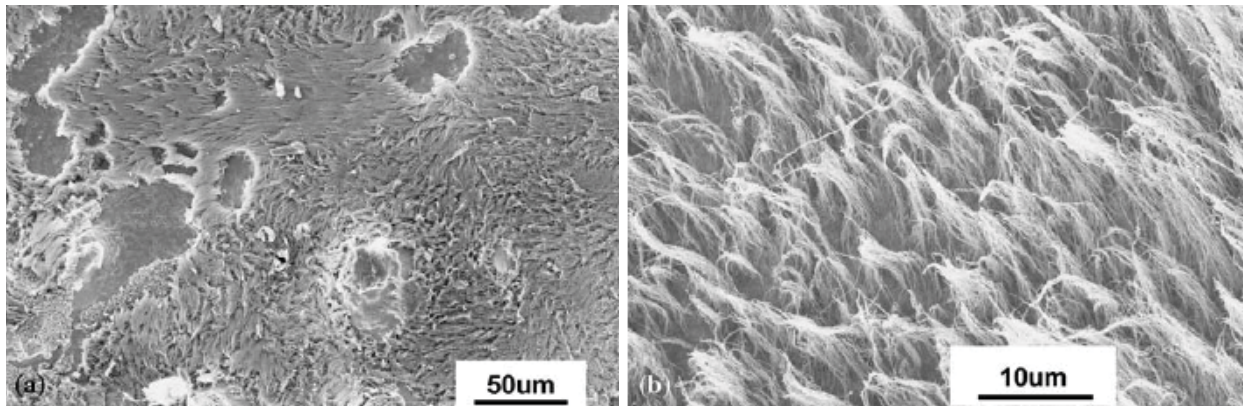


Figure 3-10. SEM images of CNTs after fracture at different magnifications [63].

When the above structures were mechanically sheared (as shown in Figure 3-10), it was found that the break of the assembly was due to the cohesive fracture of CNTs, and not the adhesive failure between CNTs and the metal adhesion layer. This test indicated that the adhesion of CNTs to the substrate was significantly improved after the transfer process. The reflow process is efficient enough to anchor the CNTs onto the metal substrate.

There are other examples of a CNT transfer process by other researchers. One particular example utilizes screen-printed adhesives to attach and transfer the CNTs to a substrate [67]; while another uses “chemical anchoring” to attach the CNTs [68].

3.3.2.2 Electrical Performance of the CNT Interconnection

The next area that is necessary to show the viability of this type of CNT interconnect technology is the electrical performance of the interconnection. In order to demonstrate the electrical

performance, a test device for electrical measurement was formed by the deposition of gold top electrodes on the surface of the aligned CNT arrays after the transfer process. Probes with a tip size of around $6\ \mu\text{m}$ were connected to the electrodes through a probe station. The electrical conductivity of the CNT arrays under the electrodes were then measured by both two- and four-probe methods. Figure 3-11 shows the measurement configurations. First, a two-probe measurement was carried out by using one probe on the top electrode and another probe on the bottom electrode (Figure 3-11a). Figure 3-11b shows the circuit diagram of this two-probe experiment. The resistance from the two-probe measurement (R_{all}) includes the resistance of the nanotubes themselves between the two electrodes (R_{CNTs}) and the contact resistance from the electrodes and wires ($R_{\text{cont}} = R_{c1} + R_{c2}$). A schematic configuration and circuit diagram of the subsequently conducted four-probe experiment are shown in Figure 3-11c and d, respectively. R_{CNTs} between the two electrodes was obtained directly from the current and voltage measured by the voltage meter. The contact resistance R_{cont} can be simply subtracted, that is, $R_{\text{cont}} = R_{\text{all}} - R_{\text{CNTs}}$.

Figure 3-12 shows the I-V characteristics of the as-transferred CNT arrays. A linear relationship between current and voltage was obtained, which indicated an ohmic contact between the CNT arrays and solders. The resistance of the transferred CNT arrays, R_{CNTs} , from the four-probe measurement was $0.0056 \pm 0.00004\ \text{X}$, while the two-probe measurement yielded $3.75 \pm 0.0047\ \text{X}$ for R_{all} , most of which can be attributed to the contact resistance from the electrodes and wires. The ohmic behavior of the curve suggests that the aligned CNTs may provide comparable performance to that of metal for chip interconnect architectures but without the material limitations presented by current state-of-the-art metal interconnects. For further application, the metal electrode/contact should be optimized.

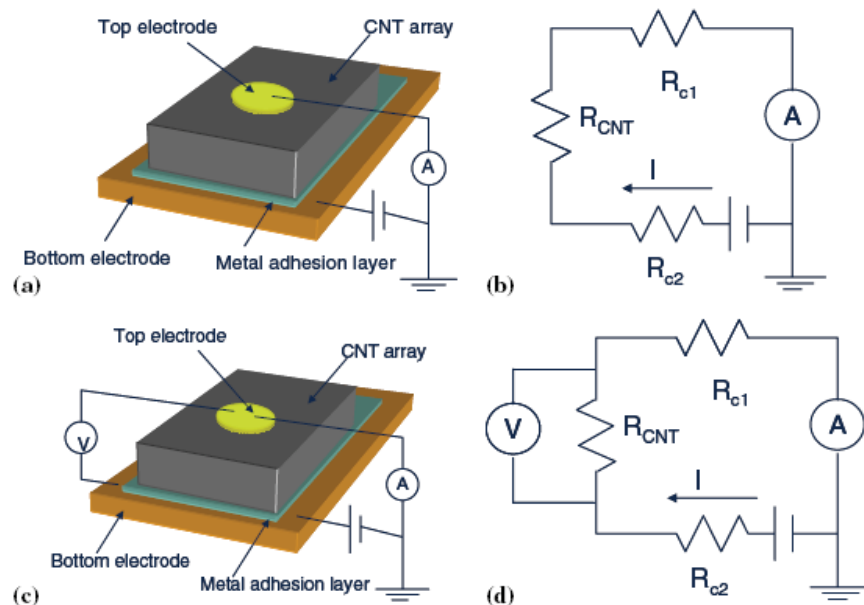


Figure 3-11. (a) Schematic configuration of the two-probe measurement and (b) circuit diagram; (c) schematic configuration of the four-probe measurement and (d) circuit diagram for CNTs demonstrated as a flip-chip interconnection method [63].

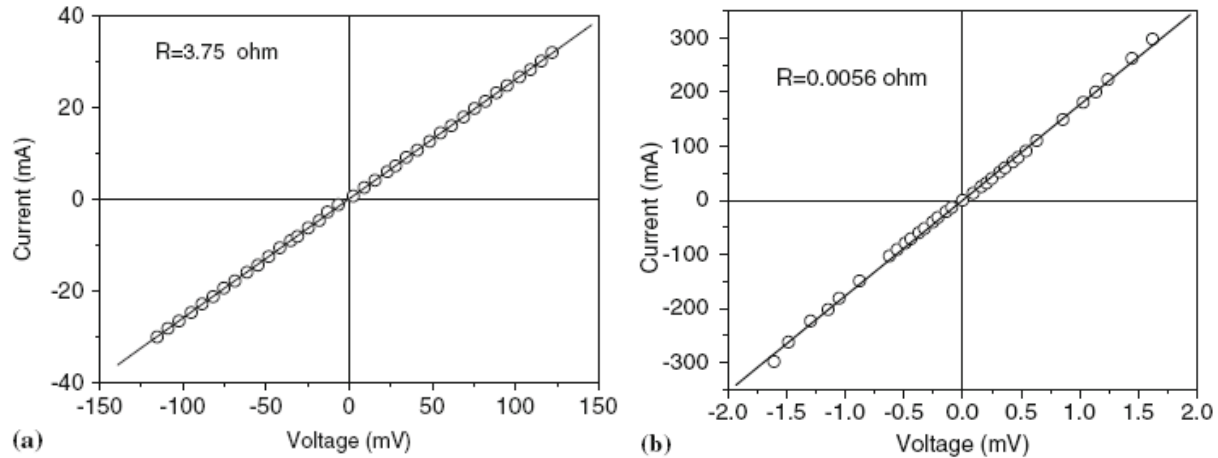


Figure 3-12. I–V characteristics of as-assembled CNT arrays by (a) two and (b) four-probe methods [63].

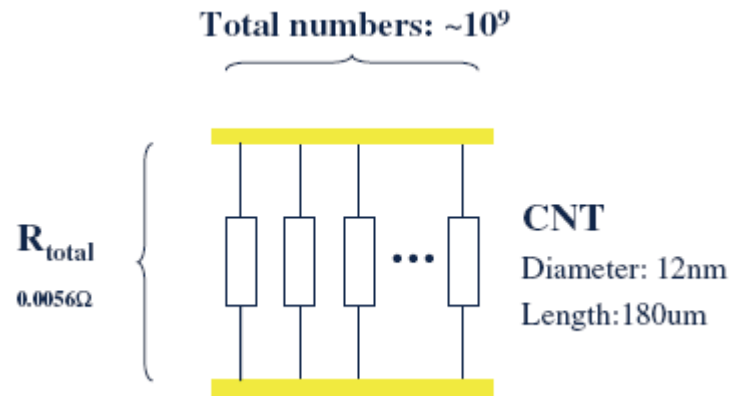


Figure 3-13. Scheme of CNT bundles between the electrodes [63].

From the electrical measurements, the resistivity of individual CNTs can be estimated by the density and diameter of the CNTs. The vertically aligned CNTs between two metal electrodes, shown in Figure 3-13, can be characterized as electrical circuits with parallel resistors since the metal electrodes are in contact with the end of each CNT and form an ohmic contact due to the high work function of the electrode metal (Pt or Au) [67]. The numbers of CNTs can be calculated from the catalyst density, as it was assumed that each catalyst particle could initiate the growth of one CNT based on the CVD mechanism. Atomic Force Microscopy (AFM) images of the catalyst on the silicon substrate indicate around 300 Fe particles per μm^2 . Therefore, the total number of CNTs under the top electrode with a 2 mm diameter is around 10^9 . The resistance for a single CNT is equal to the total resistance measured from the four-probe method multiplied by 10^9 , which is $5.6 \times 10^6 \Omega$.

These CNT arrays have been shown to be attached to copper substrates via eutectic Sn-Pb solder metal. Thermal characterization has been conducted on these structures and shown interconnect-generated negligible expansion or contraction within the temperature range used. The transferred CNT arrays showed significant adhesion to the substrates. All of the characteristics described above show that the transferred CNT arrays may be a good alternative to metal interconnects in microelectronic packaging.

3.3.2.2.1 Utilizing Thermal Compression Bonding and Adhesives

It has been demonstrated that it is possible to manufacture CNT bumps of various sizes and pitches onto a silicon chip by photolithography and plasma-enhanced chemical vapor deposition (PECVD) technologies (depicted in Figure 3-14). The chips with CNT bumps can then be bonded to ceramic substrates using thermal compression bonding or adhesives. Mechanical tests show that the bumps joined by adhesives are stronger than the thermal compression bonded bumps [68].

The overall manufacturing process of silicon chips with CNT bumps are illustrated in Figure 3-15. First, an iron (Fe) catalyst is patterned onto a silicon substrate by photolithography and evaporation techniques. The chips with CNT bumps are then bonded to substrate ceramic substrates covered with thin gold layers by both thermal compression and adhesive bonding.

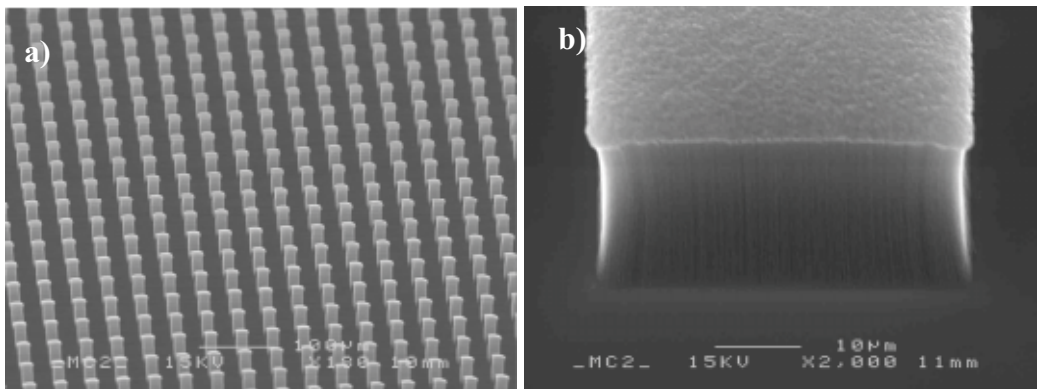


Figure 3-14. a) A scanning electron microscopy (SEM) image of an array of CNT bumps on a silicon device. The bump size is 20 μm and the pitch is 40 μm . There are totally 10,000 CNT bumps grown on the chip. The height of the bumps is approximately 30 μm . Figure b) illustrates a high magnification SEM picture of a 50 μm CNT bump showing the shape of the bump [68].

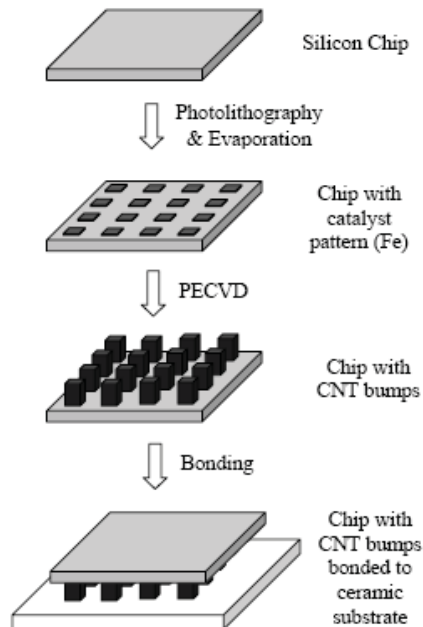


Figure 3-15. Schematic of a manufacturing process of chip with CNT bumps with the bumps attached to a ceramic substrate by using either thermal compression bonding with settings of: temperature 325°C, time = 120 seconds, and a bonding force = 20 N. The adhesive parameters were: temperature 175°C, time = 60 seconds and force = 30 N [68].

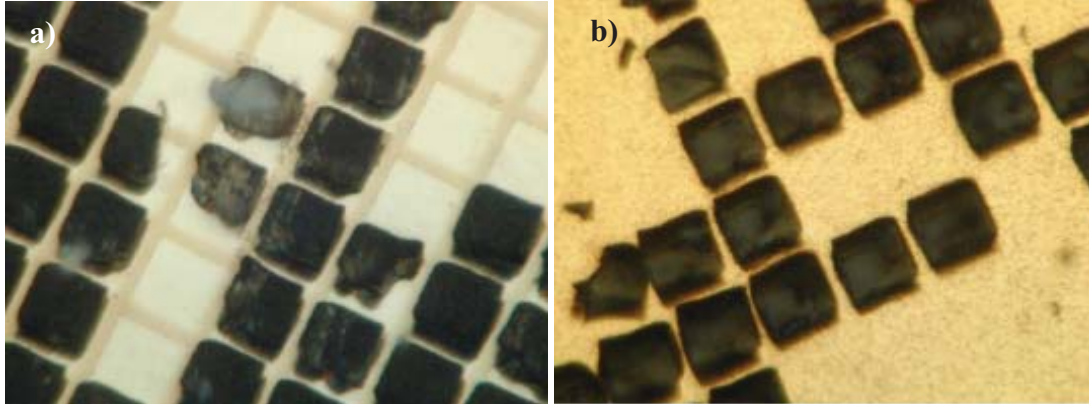


Figure 3-16. Optical photos of broken bonding interface between the gold layer of the ceramic substrate and the silicon chip: (a) The CNT bumps left on the silicon substrate. (b) The CNT bumps lift onto the thin gold film of the ceramic substrate [68].

This technique is not in production because there is no consistent strength performance shown for these two attachment techniques. The thermal compression bonds are currently weaker than the epoxy bonds, but despite their weak bonding strength, there is potential for a strong controlled process as suggested in Figure 3-16. Figure 3-16 shows the broken bonding interface between the gold layer of the ceramic substrate and the chip after a shear test. It can be clearly seen that some bumps stay on the silicon substrate while some totally lift off and stick on the gold film of the ceramic substrate. Also, some bumps are split during the shear test [68].

In summary, this technique is promising but has not been transferred to a production environment.

3.3.2.2.2 Nonconductive Adhesives/Films

With lead being the major component in solder to be eliminated because of its long recognized health threat to human beings and the environment, polymer-based conductive adhesives have been proposed as one of the lead-free candidates for interconnection. Examples of polymer-based adhesives commonly used in electronic packaging are isotropic conductive adhesives (ICAs) [69], anisotropic conductive adhesives/films (ACAs/ACFs) [70] and nonconductive adhesives/films (NCAs/NCFs) [71]. Generally, ICAs consist of an epoxy resin with high loading of conductive fillers and conduct electricity equally in all directions as shown in Figure 3-17a. ACAs/ACFs have lower conductive filler content and thus provide unidirectional conductivity in the vertical or Z direction (see Figure 3-17b). On the other hand, NCAs/NCFs do not consist of any conductive fillers, which maintain pure mechanical contacts between the bumps and pads by the compressive force (i.e., underfill).

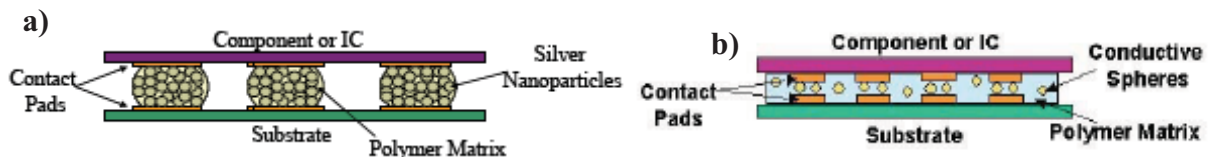


Figure 3-17. Schematic illustration of (a) ICA and (b) ACA/ACF joints [72].

Among all the conductive adhesives, NCAs/NCFs are considered most popular for flip-chip assemblies due to their low cost. Conductive joints with NCAs/NCFs provide a number of advantages compared to other adhesive bonding techniques. Size reduction of electronic devices can be realized by shrinkage of the package and the chip. Further advantages include ease of processing, good compatibility with a wide range of contact materials, and low temperature cure.

In spite of the advantages of NCAs/NCFs joints, there are still some challenging properties of NCAs/NCFs. The thermo-mechanical reliability of the NCAs/NCFs joints is poor due to high thermal stress caused by the coefficient of thermal expansion (CTE) mismatch between the epoxy materials, devices, and substrates. At the same time, the thermal conductivities of the NCAs/NCFs materials are also poor, because of the absence of conductive fillers. The heat generated at NCA/NCF joints under high current density can not be dissipated out efficiently. Therefore, the implementations of NCAs/NCFs as interconnect materials for high performance device applications, such as microprocessors and application-specific integrated circuits (ASICs) have been limited.

A technique has been developed that utilizes a small number of CNTs (0.03 wt%) dispersed into a matrix of NCAs/NCFs to increase thermal conductivity and at the same time to decrease the CTE of the NCAs/NCFs joints without degrading the electrically anisotropic conductivity of NCAs/NCFs joints [72]. The high thermal conductivity of NCAs/NCFs enables a higher current carrying capability and the lower CTE that enhances the thermo-mechanical reliability of a device. The electrical performance of this technique with NCAs/NCFs with/without CNTs was studied. The current-voltage (I-V) relationship and corresponding current-resistance (I-R) relationship of the NCAs/NCFs joints are shown in Figures 3-18 a) and b), respectively.

In addition to these performance improvements, small numbers of CNTs were found to help dissipate the heat out more efficiently and therefore enable higher current carrying capabilities of the NCAs/NCFs joints. Thermal conductivities of NCAs/NCFs with/without 0.03 wt% CNTs at different temperatures are illustrated in Figure 3-19. Notice that the 0.03 wt% CNTs resulted in an enhancement of the thermal conductivity of the NCAs/NCFs. For example, at 25°C, the thermal conductivity of the 0.03 wt% CNT-filled NCAs/NCFs was around 0.128 W/mK, compared to the unfilled NCAs/NCFs with 0.109 W/mK, an enhancement of 17%. An enhancement of 11%, 19%, and 23% was obtained at 50°C, 75°C and 100°C, respectively.

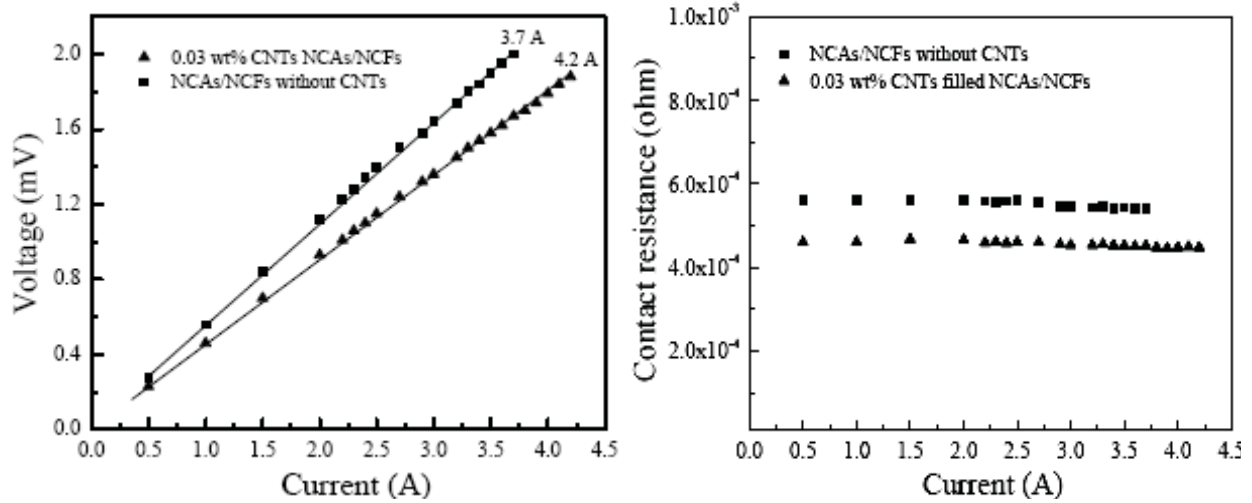


Figure 3-18. a) I-V curves of NCAs/NCFs with and without CNTs and b) contact resistance of NCAs/NCFs with/without CNTs [72].

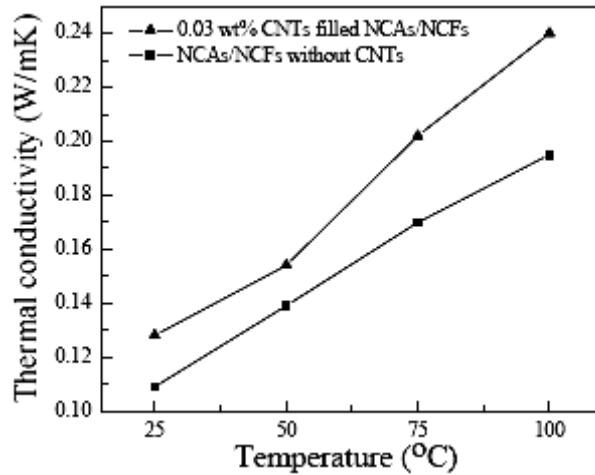


Figure 3-19. Thermal conductivities of NCAs/NCFs with and without CNTs [72].

3.3.3 Electromagnetic Shielding

Carbon nanotube structures are being developed as a cost-effective material for electromagnetic shielding of an optical transceiver module. The particular structure is made of a fine dispersion of multi-wall carbon nanotubes (MWCNTs) in a polymer matrix.

For the application of shielding material packaging for an optical transceiver module, electromagnetic interference (EMI) is one of the major concerns to maintain good signal integrity of over gigabit transmission rate [6–7]. Designing a high electromagnetic shielding package is desirable to improve the EMI performance of the optical transceiver module. It is well known that metallic packages provide an excellent shielding effectiveness (SE). The characteristics of low cost and ease of manufacturing have promoted the plastic composite package as the most suitable material for fabricating the optical transceiver modules [73–77].

However, plastics are inherently transparent to electromagnetic (EM) radiation and provide no shielding effect against radiation emissions. In order to improve the EM shielding for the plastic packaging, MWCNTs are being mixed into the plastic matrices to get adequate EM shielding properties. MWCNTs were chosen to be the fillers for their well known properties of high electrical conductivity, nanoscale diameter, high aspect ratio, and possibly strengthened mechanical properties.

Figure 3-20 illustrates that a low threshold of 5.2 wt% in the dispersed MWCNT/Polyimide composite was obtained. As a result, a high electrical conductivity and effective SE with a low loading of MWCNTs is achieved [78].

Figure 3-21 shows the SE for a dispersed MWCNT in 850 μm thickness (30% by weight). The higher measured SE represents the better electromagnetic (EM) wave shielding ability of the MWCNT/PI composite. The SE results are higher than 40 dB within the frequency range between 1 and 3 GHz, indicating that the SE is suitable for the EM shielding application of optical transceiver module packaging.

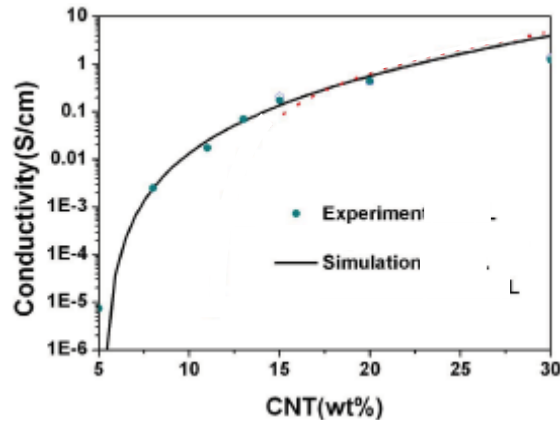


Figure 3-20. Conductivity of the MWCNT/PI composite at various weight percentage of MWCNT [78].

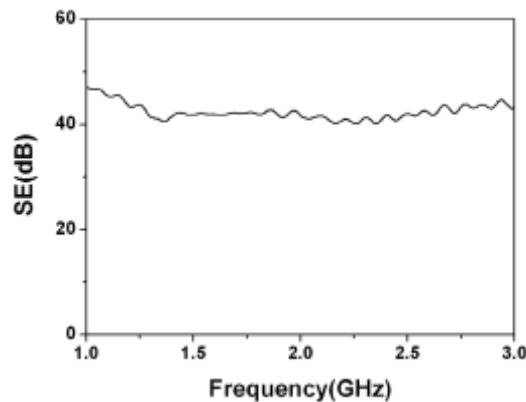


Figure 3-21. Shielding effectiveness of the MWCNT/PI composite (30 wt% MWCNT loading) [78].

4 Conclusions

The applications of carbon nanotubes (CNTs) have potential in fields such as nanotechnology, electronics, optics, materials science, and architecture. Over the years, new discoveries have led to new applications, often taking advantage of their unique electrical properties, extraordinary strength, and efficiency in heat conduction.

While CNTs have shown potential for structural applications, electromagnetic, electroacoustic, chemical, and mechanical applications, it is perhaps the applications in microelectronics that show the most promise. However, the current barriers to mass-market use of these materials include the availability of high-quality materials in commercial quantities. Joint ventures between universities and industry have helped to develop methods of producing high volume – high quality materials. As for microelectronics packaging, the United States (Georgia Tech), Korea, Taiwan and Japan are all very active.

CNTs are still in the relatively early stages of industrial development. While they are still expensive compared to a fully commoditised product, such as carbon black, the price will fall as the demand increases. The basic properties of the raw material offer a wide range of exciting applications that are beginning to be realized. As the research into these applications moves out of the lab and into industry, it is important that the supply of CNTs is consistent and of high quality. The next several years of development should see the creation of a whole new area of material and coatings science and associated commercial applications.

5 Recommendations for NASA

This is the type of technology that requires close watch for the commercial applications that could be of interest to the NEPP Program. There are a number of universities extremely active in this field with university work being paid for by commercial companies.

This technology is not mature enough to start new work in the coming fiscal year (FY); therefore, no new NEPP task is recommended for FY2010. However, since the technology is advancing at such a fast rate, it is recommended that a proposal for FY2011 or FY2012 be considered should significant commercialization occur between this year and the next year or two.

References

1. Zheng, L.X. et al. (2004). *Ultralong Single-Wall Carbon Nanotubes* **3**: 673–676.
2. Mintmire, J.W., B.I. Dunlap, and C.T. White (3 February 1992). “Are Fullerene Tubules Metallic?” *Physical Review Letters* **68**: 631–634.
3. Dekker, C. (May 1999). “Carbon nanotubes as molecular quantum wires” (PDF). *Physics Today* **52**(5): 22–28.
4. Martel, R., V. Derycke, C. Lavoie, J. Appenzeller, K. K. Chan, J. Tersoff, and Ph. Avouris (December 2001). “Ambipolar Electrical Transport in Semiconducting Single-Wall Carbon Nanotubes.” *Physical Review Letters* **87**(25): 256805.
5. Collins, P.G., and P. Avouris (December 2000). “Nanotubes for Electronics.” *Scientific American*: 67–69.
6. “Carbon Solutions, Inc.” <http://www.carbonsolution.com>

7. "CarboLex." <http://carbolex.com>.
8. Flahaut, E., R. Bacsá, A. Peigney, and C. Laurent (2003). "Gram-Scale CCVD Synthesis of Double-Walled Carbon Nanotubes." *Chemical Communications* **12**: 1442–1443.
9. Liu, L., G.Y. Guo, C. S. Jayanthi, and S.Y. Wudate (2002). "Colossal Paramagnetic Moments in Metallic Carbon Nanotubes." *Physical Review Letters* **88**(21): 217206.
10. Huhtala, M., A. Kuronen, and K. Kaski (2002). "Carbon nanotube structures: molecular dynamics simulation at realistic limit" (PDF). *Computer Physics Communications* **146**: 30.
11. Iijima, S. (1991). "Helical microtubules of graphitic carbon." *Nature* **354**: 56–58.
12. Ebbesen, T.W., and P.M. Ajayan (1992). "Large-scale synthesis of carbon nanotubes." *Nature* **358**: 220–222.
13. Guo, T. (1995). "Self-Assembly of Tubular Fullerenes," *Phys. Chem.* **99**: 10694–10697.
14. Guo, T. (1995). "Catalytic growth of single-walled nanotubes by laser vaporization," *Chem. Phys. Lett.* **243**: 49–54.
15. Walker Jr., P. L. (1959). "Carbon Formation from Carbon Monoxide-Hydrogen Mixtures over Iron Catalysts. I. Properties of Carbon Formed," *J. Phys. Chem.* **63**: 133.
16. José-Yacamán, M. (1993). "Catalytic growth of carbon microtubules with fullerene structure." *Appl. Phys. Lett.* **62**: 657.
17. Beckman, W. (April 2007). "UC Researchers Shatter World Records with Length of Carbon Nanotube Arrays." University of Cincinnati. <http://www.uc.edu/news/NR.asp?id=5700>
18. Inami, N. et al. (2007). "Synthesis-condition dependence of carbon nanotube growth by alcohol catalytic chemical vapor deposition method." *Sci. Technol. Adv. Mater.* **8**: 292.
19. Ishigami, N. et al. (2008). "Crystal Plane Dependent Growth of Aligned Single-Walled Carbon Nanotubes on Sapphire." *J. Am. Chem. Soc.* **130** (30): 9918–9924.
20. Eftekhari, A., P. Jafarkhani, and F. Moztarzadeh. (2006). "High-yield synthesis of carbon nanotubes using a water-soluble catalyst support in catalytic chemical vapor deposition." *Carbon* **44**: 1343.
21. Ren, Z. F. (1998). "Synthesis of Large Arrays of Well-Aligned Carbon Nanotubes on Glass." *Science* **282**: 1105.
22. M. Kumar and Y. Ando, (2007) "Carbon Nanotubes from Camphor: An Environment-Friendly Nanotechnology," *Journal of Physics.* **61**: 643–646.
23. Boyd, J. (Nov. 2006). "Rice chemists create, grow nanotube seeds." Rice University News and Media Relations. <http://www.media.rice.edu/media/NewsBot.asp?MODE=VIEW&ID=9070>
24. NanoLab home page, <http://www.nano-lab.com/>
25. Nanothinx home page: Nanotubes, Nanomaterials, and Nanotechnology R&D (Products), <http://www.nanotubesx.com>
26. Singer, J.M., and Grumer, J. "Carbon formation in very rich hydrocarbon-air flames. I. Studies of chemical content, temperature, ionization and particulate matter." *Seventh Symposium (International) on Combustion.* (Butterworths Scientific Publications, Ltd., London, 1959), p. 559.
27. Yuan, L., K. Saito, C. Pan, F.A. Williams, and A.S. Gordon (2001). "Nanotubes from methane flames." *Chemical physics letters* **340**: 237–241.
28. Yuan, L., K. Saito, W. Hu, and Z. Chen (2001). "Ethylene flame synthesis of well-aligned multi-walled carbon nanotubes." *Chemical physics letters* **346**: 23–28.
29. Duan, H. M., and J. T. McKinnon (1994). "Nanoclusters Produced in Flames." *Journal of Physical Chemistry* **98** (49): 12815–12818.

30. Murr, L.E., J.J. Bang, E.V. Esquivel, P.A. Guerrero, and D.A. Lopez (2004). "Carbon nanotubes, nanocrystal forms, and complex nanoparticle aggregates in common fuel-gas combustion sources and the ambient air." *Journal of Nanoparticle Research* **6**: 241–251.
31. Vander Wal, R.L. (2002). "Fe-catalyzed single-walled carbon nanotube synthesis within a flame environment." *Combust. Flame* **130**: 37–47.
32. Saveliev, A.V., Merchan-Merchan, W., and Kennedy, L.A. (2003). "Metal catalyzed synthesis of carbon nanostructures in an opposed flow methane oxygen flame." *Combust. Flame* **135**: 27–33.
33. Height, M.J., Howard, J.B., Tester, J.W., and Vander Sande, J.B. (2004). "Flame synthesis of single-walled carbon nanotubes." *Carbon* **42**: 2295–2307.
34. Sen, S., and Puri, I.K. (2004). "Flame synthesis of carbon nanofibers and nanofibers composites containing encapsulated metal particles." *Nanotechnology* **15**: 264–268.
35. Wagner, H.D. (2003), "Reinforcement," in *Encyclopedia of Polymer Science and Technology*, Vol 4, 3d Edition (J.I. Kroschwitz, Editor), Wiley-Interscience, New-York, pp. 94–115.
36. Australian Stainless Steel Development Association (ASSDA) - Home, <http://www.assda.asn.au/index.php>
37. Belluci, S. "Carbon nanotubes: physics and applications." *Phys. Stat. Sol. (c)* **2**(1): 34–47.
38. Chae, H.G., and Kumar, S. "Rigid Rod Polymeric Fibers." *Journal of Applied Polymer Science* **100**:791–802.
39. Demczyk, B.G., Wang, Y.M., Cumings, J., Hetman, M., Han, W., Zettl, A., and Ritchie, R.O. "Direct mechanical measurement of the tensile strength and elastic modulus of multiwalled carbon nanotubes." *Materials Science and Engineering* **334**:173–178.
40. Meo, M., and Rossi M. "Prediction of Young's modulus of single wall carbon nanotubes by molecular-mechanics based finite element modeling." *Composites Science and Technology* **66**:1597–1605.
41. Meo, S.B., and Andrews R. "Carbon Nanotubes: Synthesis, Properties, and Applications." *Crit. Rev. Solid State Mater. Sci.* **26**(3):145–249.
42. Ruoff, R. S. et al. (1993). *Nature* **364**, 514.
43. Palaci, I., S. Fedrigo, H. Brune, C. Klinke, M. Chen, and E. Riedo (2005). "Radial Elasticity of Multiwalled Carbon Nanotubes," *Physical Review Letters* **94**, 175502.
44. Elsevier (2006). *Carbon Based Magnetism: An Overview of the Magnetism of Metal Free Carbon-based Compounds and Materials*, edited by Tatiana Makarova and Fernando Palacio.
45. Yu, M.F., Kowalewski, T., and Ruoff, R.S. (2000). "Investigation of the Radial Deformability of Individual Carbon Nanotubes under Controlled Indentation Force," *Physical Review Letters* **85**, 1456–1459.
46. Mingo, N., Stewart, D.A., Broido, D.A., and Srivasta, D. (2008). "Phonon transmission through defects in carbon nanotubes from first principles." *Physical Review B* **77**: 033418.
47. Kahn, J. (June 2006). "Nano's Big Future," *National Geographic*.
48. Krasheninnikov, A.V., Nordlund, K., Sirvi'o, M., Salonen, E., and Keinonen, J. (2001). *Phys. Rev. B* **63**.
49. Ni, B., Andrews, R., Jacques, D., Qian, D., Wijesundara, M.B.J., Choi, Y., Hanley, L., and Sinnott, S.B. (2001) *J. Phys. Chem. B* **105**.
50. Stahl, H., Appenzeller, J., Martel, R., Avouris, Ph., and Lengeler, B. (2000). *Phys. Rev. Lett.* **85**.

51. Ziegler, J.F., Biersack, J.P., and Littmarck U. (1995). *Stopping and Range of Ions into Matter* (New York: Pergamon).
52. W. K. Hong, C. Lee, D. Nepal, K. E. Geckeler, K. Shin, and T. Lee (2006). "Radiation Hardness of the Electrical Properties of Carbon Nanotube Network Field Effect Transistors Under High-Energy Proton Irradiation," *Nanotechnology* **17**: 5675–5680.
53. Lim, Y.K., Park, B.S., Lee, S.K., and Kim, K.R. (2006) *J. Kor. Phys. Soc.* **48** 777.
54. Le Metayer, P., O. Gilard, R. Germanicus, D. Campillo, F. Ledu, J. Cazes, W. Falo, and C. Chatry (2003) *J. Appl. Phys.* **94**.
55. "Nanotubes Act As 'Thermal Velcro' To Reduce Computer-chip Heating," *Science Daily* (May 2, 2006). <http://www.sciencedaily.com/releases/2006/05/060502171803.htm>
56. Lingbo, Z., S. Yangyang, X. Jianwen, Z. Zhuqing, W. H. Dennis, C. P. Wong, "Aligned Carbon Nanotubes for Electrical Interconnect and Thermal Management," 2005 Electronic Components and Technology Conference, pp. 44–50.
57. Dujardin, E., and T. W. Ebbesen (1998). "Wetting of Single Shell Carbon Nanotubes," *Advanced Materials* **10**(17): 1472–1475.
58. Dujardin, E., T. W. Ebbesen, et al. (1994). "Capillarity and Wetting of Carbon Nanotubes," *Science* **265**: 372–374.
59. Aggarwal, A.O., P.M. Raj, I.R. Abothu, M.D. Sacks, A.A.O. Tay, and R.R. Tummala, *Proceedings of 54th Electronic Components and Technology Conference*, Las Vegas, NV, May 2004 (Piscataway, NJ: IEEE, 2004), pp. 451–460.
60. Li, S.D., Z. Yu, C. Rutherglen, and P.J. Burke (2004). *Nano Lett.* **4**: 2003.
61. Choi, W.B., E. Bae, D. Kang, S. Chae, B.H. Cheong, J.H. Ko, E. Lee, and W. Park (2004). *Nanotechnology* **15**: S512.
62. Zhang, Y., T. Ichihashi, E. Landree, F. Nihey, and S. Iijima (1999). *Science* **285**: 1719.
63. Sun, Y., L. Zhu, H. J. J. Lu, W. Wang, and C.P. Wong (2008). "A Paradigm of Carbon Nanotube Interconnects in Microelectronic Packaging," *Journal of Electronic Materials* **37**(11): 1691.
64. Zhu, L.B., Y.Y. Sun, D.W. Hess, and C.P. Wong (2006). *Nano Lett.* **6**: 243.
65. Soga, I., D. Kondo, Y. Yamaguchi, T. Iwai, M. Mizukoshi, Y. Awano, K. Yube and T. Fujii, "Carbon Nanotube Bumps for LSI Interconnect," *Proceedings of 58th Electronic Components and Technology Conference*, Lake Buena Vista, Florida, May 2008, p. 1390.
66. Lin, W., Y. Xiu, L. Zhu, K. S. Moon, and C. P. Wong (May 2008). "Assembling of Carbon Nanotube Structures by Chemical Anchoring for Packaging Applications," *Proceedings of 58th Electronic Components and Technology Conference*, Lake Buena Vista, Florida, p. 421.
67. Yang, M.H., K.B.K. Teo, W.I. Milne, and D.G. Hasko (2005). *Appl. Phys. Lett.* **87**: 253116.
68. Wang, T., M. Jönsson, E.E.B. Campbell, and J. Liu, "Development of Carbon Nanotube Bumps for Ultra Fine Pitch Flip Chip Interconnection," *Proceedings of the 2006 Electronics System Integration Technology Conference*, Dresden, Germany, p. 892.
69. Jiang, H., Moon, K., Li, Y., and Wong, C. P. (2006). "Surface functionalized silver nanoparticles for ultrahigh conductive polymer composites," *Chem. Mater.* **18**(13): 2969–2973.
70. Li, Y., Moon, K., Wong, C. P. (2006). "Enhancement of electrical properties of anisotropically conductive adhesive joints via low temperature sintering," *J. Appl. Polym. Sci.* **99**(4): 1665–1673.

71. Yim, M. J, J. S. Hwang, W. Kwon, K. W. Jang, , K. W. Paik (2003). “Highly reliable non-conductive adhesives for flip chip CSP applications,” *IEEE Trans. Elec. Pack. Manufac.* **26**(2): 150–155.
72. Jiang, H., M. J. Yim, K. Moon and C. P. Wong, “Novel Nonconductive Adhesives/Films with Carbon Nanotubes for High Performance Interconnects,” *Proceedings of the 58th Electronic Components and Technology Conference*, Lake Buena Vista, Florida, May 27–30, 2008, p. 1385.
73. Chang, C.M., J.C. Chiu, W.S. Jou, T.L. Wu, and W.H. Cheng (2006). “New Package Scheme of a 2.5Gb/s Plastic Transceiver Module Employing Multiwall Nanotubes for Low Electromagnetic Interference,” *J. Sel. Topics Quantum Electron.* **12**(5): 1025–1031.
74. Cheng (2006). “High-performance electromagnetic susceptibility of plastic transceiver modules using carbon nanotubes,” *J. Sel. Topics Quantum Electron.* **12**(6): 1091–1096.
75. Tatsuno, K., K. Yoshida, T. Kato, T. Hirataka, T. Miura, K. Fukuda, T. Ishikawa, M. Shimaoka, and T. Ishii (1999). “High-performance and low cost plastic optical modules for access network system applications,” *J. Lightwave Technol.* **17**(7): 1211–1216.
76. Fukuda, M., F. Ichikawa, Y. Shuto, H. Sato, Y. Yamada, K. Kato, S. Tohno, H. Toba, T. Sugie, J. Yoshida, K. Suzuki, O. Suzuki, and S. Kondo (1999). “Plastic module of laser diode and photodiode mounted on planar lightwave circuit for access network,” *J. Lightwave Technol.* **17**(7): 1585–1590.
77. Cheng, W.H., W.C. Hung, C.H. Lee, G.L. Hwang, W.S. Jou, and T.L. Wu (2004). “Low cost and low electromagnetic interference packaging of optical transceiver modules,” *J. Lightwave Technol.*, **22**(9): 2177–2183.
78. Chiu, J.C., C. M. Chang, J. W. Lin and W. H. Cheng, “High Electromagnetic Shielding of Multi-Wall Carbon Nanotube Composites Using Ionic Liquid Dispersant,” *Proceedings of the 58th Electronic Components and Technology Conference*, Lake Buena Vista, Florida, May 27–30, 2008, p. 427.